ELECTROPLATING BASED CIGS TECHNOLOGY FOR ROLL-TO-ROLL MANUFACTURING

B. M. Başol, M. Pinarbasi, S. Aksu, J. Wang, Y. Matus, T. Johnson, Y. Han, M. Narasimhan and B. Metin
SoloPower Inc.
5981 Optical Court, San Jose, CA 95138

ABSTRACT: A low cost electrodeposition technique was used in conjunction with an annealing/crystallization process step to grow CIGS absorber layers on flexible metal foil substrates. Small area cells with close to 14% efficiency and large area devices with efficiencies exceeding 11% were fabricated. Roll-to-roll electrodeposition technique was shown to yield excellent compositional control and thickness uniformity for CIGS precursors. Large area solar cells were used in fabrication of modules with about 1 m^2 aperture area and over 90W output. Flexible packaging was also investigated for the CIGS devices. Damp heat testing showed good stability for both glass based rigid and flexible packages.
Keywords: CIGS, electrodeposition, flexible substrate

1 INTRODUCTION

CIGS is a leading thin film PV material with demonstrated small area solar cell efficiencies close to 20% [1]. Despite this success in achieving high conversion efficiencies, however, commercialization of CIGS technologies has not been rapid. One reason for this is the difficulty of scaling up the rather expensive vacuum-based CIGS manufacturing approaches while keeping the cost structure competitive with dominant wafer Si technologies.

Electrodeposition is a low cost method that was succesfully applied to CdTe and HgCdTe film growth for photovoltaic applications in early 1980's [2]. A wide range of processing approaches employing electrodeposition have also been explored for CIS and CIGS film formation during the last two decades. These approaches include; i) electrodeposition of thin Cu and In layers forming a Cu/In precursor stack and reacting this metallic stack with gaseous Se species to form the compound [3], ii) electrodeposition of a Cu/In/Se stack on a substrate and rapid thermal annealing of the stack to form CIS [4], iii) electrodeposition of In-Ga [5], Cu-Ga [6] or Cu-In-Ga [7] metal alloys to form precursor layers and reacting these precursor layers to form the compound, iv) electrodeposition of In-Se and Cu-Se on a substrate forming a stacked precursor such as a Cu/In-Se/Cu-Se structure and annealing the structure in inert atmosphere to form CIS [8], and v) one step electrodeposition of CIS or CIGS compound films and subjecting them to a high temperature crystallization step to improve their photovoltaic properties [9]. Reader is referred to Lincot et al. for a more detailed review of these various electrodeposition approaches [10].

As can be seen from the berief discussion above electrodeposition is a versatile method with ability to yield thin films of metals, metal alloys and compounds which may be used in a wide variety of precursor layer structures. Electrodeposition equipment is low cost. The process is energy efficient since it is typically carried out at low temperatures. Materials utilization in electrodeposition processes can be close to 100% if stable electrolytes with long lifetime are employed. Electrodeposition is also suitable for high throughput manufacturing. Despite all these attractive features, however, electrodeposition has not yet been scaled up for manufacturing CIGS-type solar cells and modules. This is partly due to the complex nature of the CIGS material and partly due to some of the unique challenges associated with the electrodeposition approach. First of all, unlike CdTe which can easily be processed as a single phase material which yields high efficiency devices, photovoltaic properties of CIGS are sensitive to its phase content which, in turn, depends on its composition. Therefore, any thin film deposition technology employed for manufacturing CIGS solar cells needs to have the ability to control the Cu/(In+Ga) and Ga/(Ga+In) molar ratios in the deposited layers, both in macro-scale and micro-scale. Since much of the prior electrodeposition work on CIGS has been laboratory scale research, such compositional control has not yet been demonstrated on large area substrates with a truly scalable process. Furthermore, Ga inclusion in CIGS layers has historically been a challenge for researchers due to the fact that Ga plating potential is much higher than the deposition potentials of other metallic constituent of the compound (the reduction potential of Ga^{3+} is -0.53 V, compared to -0.34 V for In^{3+}, and +0.34 for Cu^{+}, with respect to Normal Hydrogen Electrode-NHE), causing Ga to deposit very inefficiently. Scaling up of the electrodeposition processes requires careful hardware design to provide uniform plating current density distribution as well as uniform electrolyte flow over large area substrates so that the thickness uniformity and the compositional uniformity of the deposited layers may be assured.

In this paper we report on the results of a work which was initiated to develop and demonstrate an electrodeposition based CIGS technology that can be scaled up to manufacture large area solar cells and modules.

2 EXPERIMENTAL

2.1 CIGS film growth

CIGS layers were formed on 25-75 μm thick flexible stainless steel foil substrates. After cleaning of the substrates and sputter deposition of a Mo-based contact layer, a precursor film containing preselected amounts of Cu, In, Ga and Se was electrodeposited on the contact layer. Initial development work was carried out on 6"x8" size substrates in a batch system to collect the deposition uniformity and plating bath stability data. For roll-to-roll

processing, an electroplating tool with the capability to handle 13.5" wide foil substrates (web) was employed. The minimum lenght of the stainless steel web was 500 ft. An RTP-type annealing/crystallization process step was carried out to convert the electrodeposited precursor films into device quality CIGS layers. The typical temperature range employed in this process step was 500-550 °C, although CIGS film formation was achieved in a wider temperature range of 450-600 °C. The thickness of the CIGS layers was in the range of 1-2 μm.

2.2 Cell fabrication

A typically 100 nm thick CdS buffer layer was deposited on the CIGS absorber by the chemical bath deposition approach. An i-ZnO/TCO stack was then sputter deposited over the buffer layer to yield a sheet resistance value in the range of 40-60 Ω/□. Aluminum/Ni finger patterns were deposited by e-beam evaporation on small area devices. For cells larger than 50 cm^2 area, a grid pattern was screen printed using a Ag-base paste with a cure temperature below about 250 °C.

2.3 Packaging and module fabrication

Solar cells with a nominal area of 100 cm^2 were interconnected using 2.5 mm wide copper ribbons to form strings. Modules with glass/glass and glass/back-sheet configurations were fabricated using standard vacuum lamination equipment. To form flexible structures, solar cells were packaged in between two flexible transparent sheets with moisture barrier films. The transparent flexible sheets with multi-layer moisture barrier coatings were provided by Pacific Northwest National Laboratory (PNNL) [11].

2.4 Measurements

Compositional analysis of the films was carried out by ICP on solutions prepared by cutting coupons from the various regions of the large area samples and then chemically dissolving these coupons. X-ray fluorescence was also employed for compositional measurements as a non-destructive method on parts of the substrates where solar cells were later formed. I-V characteristics of the finished devices were measured at SoloPower and NREL under standard AM1.5 conditions. For damp heat testing, the packaged cell and module structures were placed in a humidity chamber under the conditions of 85 °C and 85% relative humidity. Their performance was measured at intervals after removing them from the test chamber.

3 RESULTS AND DISCUSSION

3.1 Electrodeposited layers

As discussed previously, one of the most important requirements for successful application of an electrodeposition technique to CIGS absorber formation is the demonstration of the ability of the technique to control the composition of the deposited films in a reliable and repeatable manner. Figure 1 shows the Ga/(Ga+In) molar ratio data collected from the electrodeposited layers by ICP measurements during a period of 95 days. The target in this experiment was a molar ratio of 0.3. The electrolyte and the process conditions were kept unchanged during the whole test period. The data of Figure 1 demonstrates that the electrodeposition process of this work has the capability to include Ga in the deposited films in a reliable and repeatable manner.

Figure 2 shows the Cu/(Ga+In) molar ratio data collected from the same plated samples during the same 95 day period. The target ratio in this case was 0.8 and as can be seen from the data, this ratio was controlled between the values of 0.76 and 0.84 as measured by ICP. This is within the accuracy band of the measurement method and therefore the results demonstrate a good ability for the technique to control composition. It should be noted that for the two excursion points in the data of Figure 2, the measurement instrument was found to be faulty.

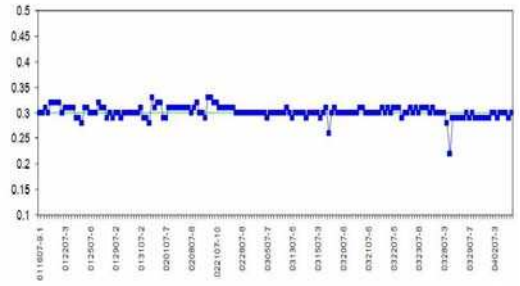

Figure 1: The Ga/(Ga+In) molar ratio data collected from samples electroplated during a period of 95 days

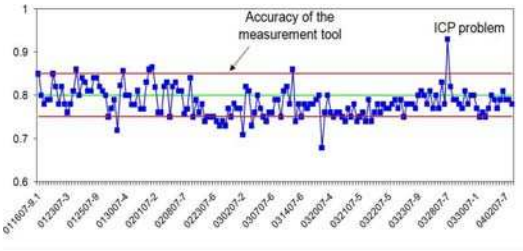

Figure 2: The Cu/(Ga+In) molar ratio data collected from samples electroplated during a period of 95 days

3.2 Uniformity of the roll-to-roll process

In addition to the repeatability and robustness of the electrodeposition process in terms of its compositional control, experiments were also carried out with the roll-to-roll electroplating tool to demonstrate that film thickness and the stoichiometry is uniform throughout a large area substrate. In one experiment a 13.5" wide and 400 ft long foil substrate was continuously processed through the roll-to-roll electroplating system and then the deposited film thickness, the Cu/(Ga+In) ratio and the Ga/(Ga+In) molar ratio were measured across the 12" wide section of the web as well as along the web, at 100 ft intervals. The thickness of the deposit was found to be within 10% of the target value. Figures 3a and 3b respectively show the Cu/(Ga+In) molar ratio data collected across the width of the foil substrate, at the beginning of the web, and at the location 300ft away from the beginning of the web. Although the data for the Ga/(Ga+In) molar ratio is not presented here, both the Cu/(Ga+In) molar ratio and the Ga/(Ga+In) molar ratio

were found to be within +/- 8 % of their respective target values throughout the 400 ft long substrate.

3.3 CIGS layers

CIGS layers were of good crystalline quality and displayed a preferred <112> orientation. The grain size was found to be a strong function of the Ga content of the film as well as the details of the crystallization process step. Figure 4 is a top view SEM taken from a CIGS layer and it shows well formed grains with a grain size of larger than 1 μm. The cross sectional SEM of Figure 5 was taken from a film formed at the high end of the temperature process window and it shows grain structure to be columnar with grains extending all the way to the contact layer.

3.4 Solar cells

The illuminated I-V characteristics of a 0.48 cm^2 area solar cell fabricated on a stainless steel foil substrate is shown in Figure 6. The Al/Ni grid pattern was evaporated through a shadow mask on this device. The total area efficiency is 13.76% with an open circuit voltage value near 550 mV. For large area flexible devices both 50 cm^2 and 100 cm^2 designs were fabricated. NREL confirmed a total area conversion efficiency of 11.39 % for a 51.87 cm^2 device with V_{oc}, J_{sc} and FF values of 0.5613 V, 31.29 mA/cm^2 and 64.85 %, respectively. Figure 7 shows the illuminated I-V characteristics of a 101 cm^2 area device with a total area conversion efficiency of 11.17 %. The open circuit voltage is close to 570 mV. The fill factor is lower than that of the smaller cells primarily due to the un-optimized sheet resistance of the screen printed contact pattern. Also the shadowing loss of the screen printed contact is higher than that of the evaporated contact employed for the small area devices.

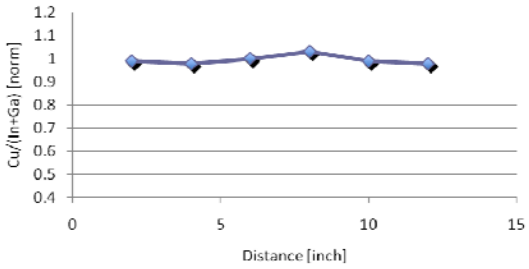

Figure 3a: The Cu/(Ga+In) molar ratio measured across a 13.5" wide and 400 ft long foil substrate at a location near the beginning of the web

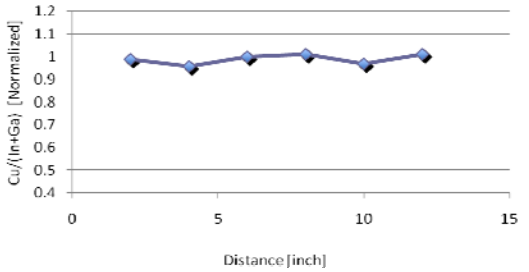

Figure 3b: The Cu/(Ga+In) molar ratio measured across a 13.5" wide and 400 ft long foil substrate at a location 300ft from the beginning of the web

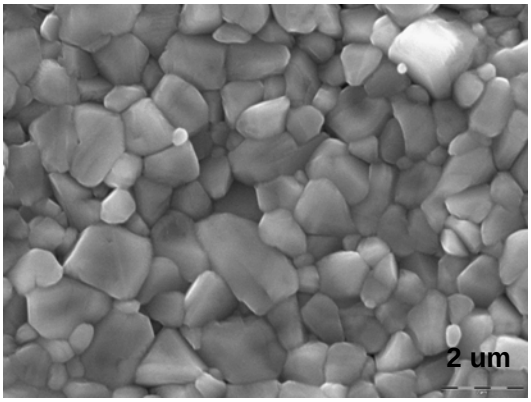

Figure 4: Top view SEM of a CIGS layer grown on a metal foil substrate

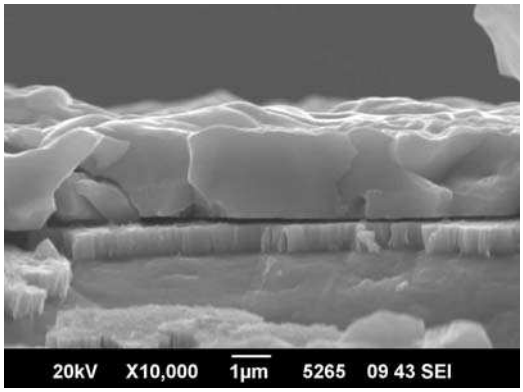

Figure 5: Cross sectional SEM of a CIGS layer grown on a metal foil substrate at elevated temperatures

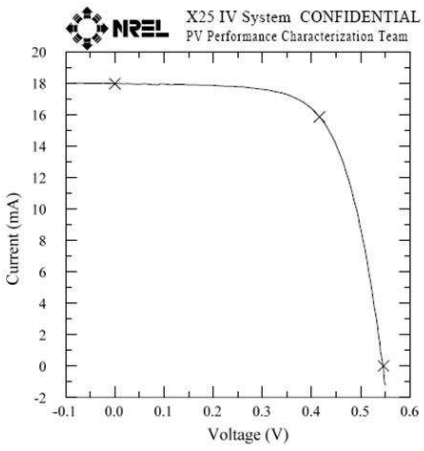

Figure 6: Illuminated I-V characteristics of a 0.48 cm^2 area device

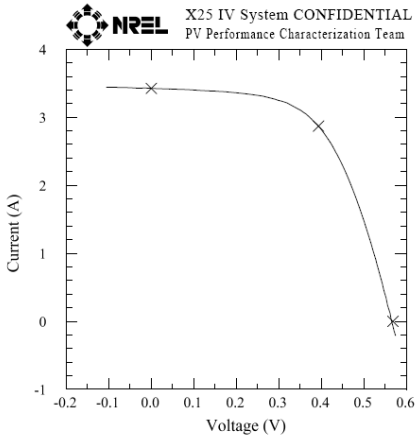

V_{oc} = 0.5682 V
I_{sc} = 3.4244 A
J_{sc} = 33.902 mA/cm^2
Fill Factor = 58.00 %

I_{max} = 2.8697 A
V_{max} = 0.3933 V
P_{max} = 1.1287 W
Efficiency = 11.17 %

Figure 7: Illuminated I-V characteristics of a 101 cm^2 area device

3.3 Modules

Figure 8 shows the illuminated I-V characteristics of a module fabricated by bussing and packaging ten cell strings. Each string contained ten interconnected cells of a nominal area of 102 cm^2. The total aperture area of the module was 1.05 m^2. After lamination and framing the module was sent to NREL for measurement. As can be seen from the data of Figure 8, the total power output was measured to be 94.34 W with V_m and I_m values of about 37.3 V and 2.53 A, respectively .

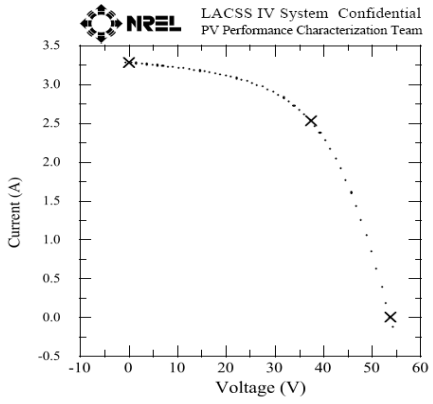

V_{oc} = 53.67 V
I_{sc} = 3.275 A
Fill Factor = 53.7%
Efficiency = 8.96%

V_{max} = 37.31 V
I_{max} = 2.529 A
P_{max} = 94.34 W

Device Dimensions = 113.0 x 93.2 cm

Figure 8: The illuminated I-V characteristics of a 1.05 m^2 area module fabricated using 100 flexible interconnected CIGS cells

3.4 Damp heat tests

The results of over 1000 hrs of damp heat test for glass/glass and glass/foil rigid package structures are shown in Figure 9. As can be seen from this data, stable performance for electrodeposition-based CIGS devices may be achieved provided that measures are taken to avoid moisture penetration into the device package. Figure 10 shows the damp heat test results for a 25 cm^2 area device packaged in a flexible structure where the cell was sandwiched between two transparent foils with multi-layer moisture barrier films [11]. The device performance is stable for over 1000 hrs under damp heat conditions. It should be noted that reference cells placed in the same test chamber without any protective package typically loose at least 60% of their power output after 1000 hrs of exposure. Most of the loss typically comes from lower fill factors and short circuit current values.

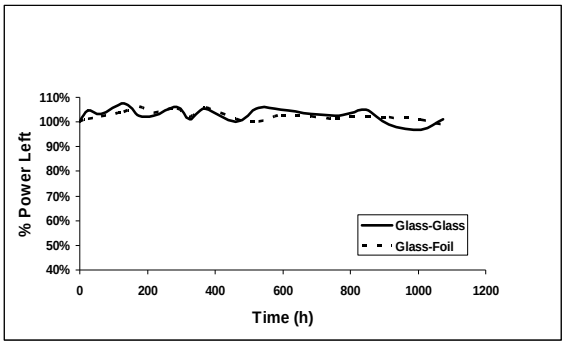

Figure 9: Power output of devices packaged in glass/glass and glass/foil structures during damp heat test performed under 85 °C/85% relative humidity conditions

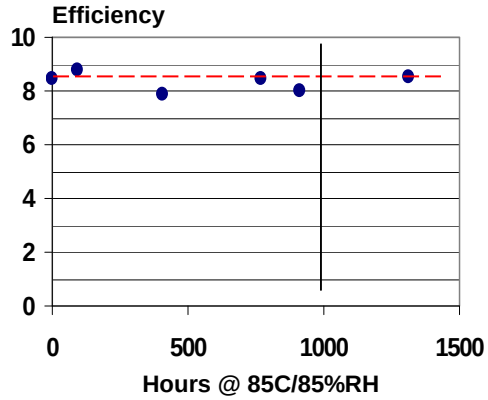

Figure 10: Damp heat test data collected from a 25 cm^2 area cell packaged in a flexible structure with moisture barrier coatings [11]

4 CONCLUSIONS

An electrodeposition based CIGS technology was developed and transferred to roll-to-roll manufacturing tools. Thickness uniformity and compositional control capability of the method was demonstrated on several hundred feet long substrates. Large area cell efficiencies

of over 11% were obtained. Large area modules with over 94 W output were fabricated. Presently, efforts are concentrated on finalizing the manufacturing factory and increasing the large area cell efficiencies towards the 14% level which was achieved for small area devices.

5 ACKNOWLEDGEMENTS

Authors thank H. Talieh, J. Ashjaee, R. Langley, R. Noufi and the whole SoloPower team for their contributions to the reported work. Partial funding by DOE/NREL through Subcontract No. NAT-7-77015-10 is gratefully acknowledged.

6 REFERENCES

[1] I. Repins et al., Progress in Photovoltaics: Research and Applications 16 (2008) 235.
[2] B. Basol, Solar Cells 23 (1988) 69.
[3] V. Kapur et al., Solar Cells 21 (1987) 65.
[4] H. Fritz et al., Thin Solid Films 247 (1994) 129.
[5] J. Zank et al., Thin Solid Films 286 (1996) 259.
[6] R. Friedfeld et al., Solar Energy Materials and Solar Cells 31 (1999) 163.
[7] M. Ganchev et al., Thin Solid Films 511-512 (2006) 325.
[8] A. Fernandez et al., Solar Energy Materials and Solar Cells 52 (1998) 423.
[9] R. Bhattacharya et al., Solar Energy Materials and Solar Cells 55 (1998) 83.
[10] D. Lincot et al., Solar Energy 77 (2004) 725.
[11] L. Olsen et al., SPIE Symposium on Solar Energy and Applications: Reliability of PV cells, modules, components and systems, San Diego, August 10-14, 2008.